Overexpression of the class D MADS-box gene *Sl-AGL11* impacts fleshy tissue differentiation and structure in tomato fruits

Baowen Huang[1,2,3], Jean-Marc Routaboul[1,2], Mingchun Liu[1,2], Wei Deng[3], Elie Maza[1,2], Isabelle Mila[1,2], Guojian Hu[1,2], Mohamed Zouine[1,2], Pierre Frasse[1,2], Julia T. Vrebalov[4], James J. Giovannoni[4], Zhengguo Li[3,*], Benoît van der Rest[1,2,*] and Mondher Bouzayen[1,2]

[1] Université de Toulouse, Institut National Polytechnique de Toulouse-Ecole Nationale Supérieure Agronomique, Unité Mixte de Recherche 990 Génomique et Biotechnologie des Fruits, Castanet-Tolosan, F-31326, France

[2] Institut National de la Recherche Agronomique, Unité Mixte de Recherche 990 Génomique et Biotechnologie des Fruits, Castanet-Tolosan, F-31326, France

[3] Genetic Engineering Research Centre, School of Life Sciences, Chongqing University, Chongqing, 400044, PR China

[4] Boyce Thompson Institute and USDA-ARS Robert W. Holley Center, Cornell University campus, Ithaca, NY 14853, USA

* Correspondence: benoit.van-der-rest@ensat.fr or zhengguoli@cqu.edu.cn

Abstract

MADS-box transcription factors are key elements of the genetic networks controlling flower and fruit development. Among these, the class D clade gathers *AGAMOUS*-like genes which are involved in seed, ovule, and funiculus development. The tomato genome comprises two class D genes, *Sl-AGL11* and *Sl-MBP3*, both displaying high expression levels in seeds and in central tissues of young fruits. The potential effects of *Sl-AGL11* on fruit development were addressed through RNAi silencing and ectopic expression strategies. *Sl-AGL11*-down-regulated tomato lines failed to show obvious phenotypes except a slight reduction in seed size. In contrast, *Sl-AGL11* overexpression triggered dramatic modifications of flower and fruit structure that include: the conversion of sepals into fleshy organs undergoing ethylene-dependent ripening, a placenta hypertrophy to the detriment of locular space, starch and sugar accumulation, and an extreme softening that occurs well before the onset of ripening. RNA-Seq transcriptomic profiling highlighted substantial metabolic reprogramming occurring in sepals and fruits, with major impacts on cell wall-related genes. While several *Sl-AGL11*-related phenotypes are reminiscent of class C MADS-box genes (*TAG1* and *TAGL1*), the modifications observed on the placenta and cell wall and the *Sl-AGL11* expression pattern suggest an action of this class D MADS-box factor on early fleshy fruit development.

Key words: Cell wall, fleshy tissue, fruit development, MADS, tomato.

Introduction

MADS-box genes belong to a large family of transcription factors present in all plant species and are reported to control development of organs such as flowers, ovules, seeds, leaves, and roots (Riechmann and Meyerowitz, 1997; Ng and Yanofsky, 2001; De Folter *et al.*, 2006; Deng *et al.*, 2012; Xu *et al.*, 2016). In flower development, they have

been subdivided into five different classes (A, B, C, D, and E genes) that are important for specifying sepals (A, E), petals (A, B, E), stamens (B, C, E), carpels (C, E), and ovules (D, E). Several MADS-box genes have been reported to affect tomato fruit development and ripening: class A *FUL1* and *FUL2* (Bemer *et al.*, 2012; Shima *et al.*, 2014), class C *TAG1* (Pnueli *et al.*, 1994) and *TAGL1* (Itkin *et al.*, 2009; Vrebalov *et al.*, 2009; Giménez *et al.*, 2010), class E *RIN*, *TM29*, and *MADS1* (Vrebalov *et al.*, 2002; Ampomah-dwamena *et al.*, 2002; Dong *et al.*, 2013), and non-classified *FYFL* (Xie *et al.*, 2014). These transcription factors may directly or indirectly interact with target DNA as complexes of varying composition to regulate fruit development and ripening (Karlova *et al.*, 2014). Recently, ChIP approaches uncovered target genes for some of the MADS-box proteins; that is, RIN binds to at least 241 direct targets, resulting in both their positive and negative regulation. Consistent with its role in climacteric fruit ripening, RIN binds to genes involved in ethylene biosynthesis (*ACS2* and *ACS4*) and perception (*NR*), as well as cell wall-remodeling genes (Martel *et al.*, 2011; Qin *et al.*, 2012; Fujisawa *et al.*, 2013; Zhong *et al.*, 2013). In addition, the FUL1/FUL2/RIN complex can bind to different target genes such as those involved in the flavonoid and carotenoid biosynthesis pathways (Fujisawa *et al.*, 2013; Zhong *et al.*, 2013).

TAG1 and *TAGL1*, the two tomato members of the class C MADS-box gene family, are orthologous to Arabidopsis *AGAMOUS* (*AG*) and *SHATTERPROOF1/2* (*SHP1/SHP2*), respectively. *TAG1* RNAi-mediated down-regulation led to stamen defects and loss of floral organ determinacy, as evidenced by the nested flowers-in-flower (Pnueli *et al.*, 1994) or fruit-in-fruit phenotypes (Pan *et al.*, 2010). *TAGL1* down-regulation resulted in ripening inhibition and reduced pericarp thickness (Itkin *et al.*, 2009; Vrebalov *et al.*, 2009; Giménez *et al.*, 2010). Double RNAi silencing of tomato *TAG1* and *TAGL1* indicated that these two genes have both redundant and divergent functions in regulating carpel identity and pollen development (Pan *et al.*, 2010; Giménez *et al.*, 2016). This tomato subfunctionalization of class C MADS-box genes is reminiscent of Arabidopsis and other Angiosperms where *AG*, *SHP1*, and *SHP2* exert overlapping functions such as floral meristem determinacy and the ability to promote reproductive organ development (Dreni and Kater, 2014), while *SHP1* and *SHP2* specifically control valve margin identity and development of the dehiscence zones (Liljegren *et al.*, 2000).

Sl-AGL11 and *Sl-MBP3* are highly related to the *AGAMOUS* family and belong to the class D MADS-box genes. They are putative orthologs of the Arabidopsis *SEEDSTICK* (*STK*) gene (Pinyopich *et al.*, 2003; Mizzotti *et al.*, 2012) and of the petunia *Floral Binding Proteins 11* and *7* (*FBP11* and *FBP7*) genes (Angenent *et al.*, 1995; Colombo *et al.*, 1995). Simultaneous down-regulation of *FBP7/FBP11* by co-suppression (Angenent *et al.*, 1995) or by transposon insertion (Heijmans *et al.*, 2012) leads to carpel-like structures instead of ovules and to aberrant seed development, indicating that the *FBP7/11* gene pair has a unique function in seed development. Redundantly with other *AG* clade members, they also specify ovule identity (Pinyopich *et al.*, 2003; Heijmans *et al.*, 2012). In Arabidopsis, *STK* mutant shows defects in ovule development including reduced fruit and seed size, and an abnormal funiculus that disturbs seed spacing and dispersal at fruit maturation (Pinyopich *et al.*, 2003). In the seed coat, STK protein also regulates cell wall strengthening and flavonoid accumulation. For instance, it may repress *BAN/ANR*, the main biosynthetic gene leading to proanthocyanidin (PA) accumulation and control endothelium development and differentiation (Mizzotti *et al.*, 2014). STK has also been reported to repress some genes involved in pectin maturation and glucomannan or cellulose deposition in seed coat or columella (Ezquer *et al.*, 2016).

Recent work on fruit crop species provided evidence for the potential impact of class D MADS-box genes on fruit quality traits. It was shown that the palm tree *STK* ortholog, *SHELL*, controls the development of the thick coconut-like shell surrounding the kernel with consequences on oil yield and composition (Singh *et al.*, 2013). In grapevine, an *STK* ortholog, *VviAGL11*, has been shown to be a key gene to control fruit seedlessness in addition to its previously described roles in ovule patterning (Mejía *et al.*, 2011; Ocarez and Mejía, 2016; Malabarba *et al.*, 2017). In addition, *Sl-AGL11*, the putative *Vvi-AGL11* ortholog, was reported potentially to control seed formation (Ocarez and Mejía, 2016). However, these observations were based on the phenotype displayed by tomato T0 RNAi lines, and the global impact on fruit development has not been documented.

To address further the functional significance of *Sl-AGL11*, formerly called *Le-TAGL11* or *Sl-TAGL11* (Itkin *et al.*, 2009; Vrebalov *et al.*, 2009), both overexpressing and down-regulated tomato lines were generated and analyzed. To uncover further the physiological significance of *Sl-AGL11*, we report here that the ectopic expression of this gene results in dramatic modifications in flower and fruit organization. In particular, the conversion of the sepals into a carpel-like fleshy organ, and the enhanced fruit softness and sugar content are indicative of major metabolic reorientations as validated by genome-wide gene expression profiling.

Materials and methods

Plant materials

Tomato (*Solanum lycopersicum* cv MicroTom) seeds were sown on 0.5× Murashige and Skoog (MS) medium (pH 5.9) with 0.8% (w/v) agar and were transferred to soil after 2 weeks and maintained in a culture chamber (14 h day/10 h night cycle, 25/20 °C day/night temperature, 80% relative humidity). Development and ripening measurements refer to days post-anthesis (DPA) or breaker (BR) stage. Flowers at the 'anthesis stage' were determined according to the change of petal color (deep yellow) and to a slight elongation observed either in wild-type (WT), *Sl-AGL11* RNAi, or *Sl-AGL11OE* plants, which coincided with the acquisition of the pollination capacity. Fruits at the BR stage were determined according to the yellow color change observed on mature green fruits.

Pollination assay

Flower buds were emasculated before dehiscence of anthers according to Wang *et al.* (2005). Hand cross-pollination was performed on emasculated flowers 1 d prior to anthesis.

Plant transformation

Transgenic plants with altered *Sl-AGL11* expression were obtained via *Agrobacterium*-mediated transformation as described in Hao *et al.* (2015), and transformed lines were selected on kanamycin (70 mg l^{-1}).

For *Sl-AGL11* down-regulation, a construct enabling RNAi silencing was designed using the pHELLSGATE-12 system (Invitrogen). The *Sl-AGL11* 3′ end was introduced in sense and antisense orientation after amplification with the forward 5′-ACATGATGGAAACTGCACTACC-3′ and reverse 5′-GCCCCAAATTTTAGGAAATGATGC-3′ primers and intermediary cloning into the pDONOR207.

For *Sl-AGL11* overexpression, the full length was amplified by PCR with the forward 5′-ATGGGTCGAGGAAAGATAGAG-3′ and reverse 5′-TTACCTTTTGTGATCAGGAGACAA-3′ primers and inserted into the *Sma*I site of a modified 35S-PLP100 vector containing the *Cauliflower mosaic virus* (CaMV) 35S promoter and the Nos terminator (Hu *et al.*, 2014). Clone orientation and sequence were confirmed by sequencing before introduction into the C58 *Agrobacterium* strain.

RNA extraction and quantitative real-time PCR (qPCR)

Five individual fruits at each developmental stage were harvested and frozen in liquid nitrogen. Total RNA samples were isolated using Trizol (Invitrogen) according to the manufacturer's instructions and were treated with DNase I (Invitrogen). The first-strand cDNA synthesis was performed using 1 µg of total RNA with an Omniscript Reverse Transcription kit (Qiagen). qPCR was performed in a 10 µl reaction volume using the SYBR Green PCR Master Mix on an ABI PRISM 7900HT sequence detection system (Applied Biosystems). Primers used for PCR amplification are listed in Supplementary Table S2 at *JXB* online. Three independent RNA isolations were used for cDNA synthesis and each cDNA sample was subjected to RT-PCR analysis in triplicate. Actin was used as the internal reference (Løvdal and Lillo, 2009).

Subcellular localization of Sl-AGL11 proteins

A *Sl*-AGL11–green fluorescent protein (GFP) C-terminal fusion was generated and introduced into a pGreen vector backbone containing the 35S CaMV promoter. A pGreen-GFP empty vector was used as a cytoplasmic control. Alternatively, a yellow fluorescent protein (YFP) N-terminal fusion was achieved by introducing *Sl-AGL11* in the pEarlyGate104 vector (Earley *et al.* 2006). The nucleus control 35S:RFP-N7 was constructed including the N7 nuclear targeting signal in the expression clone pH7WGR2,0. Tobacco (*Nicotiana tabacum*) BY-2 cell protoplasts were transfected according to Leclercq *et al.* (2005) and fluorescence was followed by confocal microscopy as described previously (Audran-Delalande *et al.*, 2012).

Ethylene and 1-MCP treatment

Ethylene and 1-methylcyclopropene (1-MCP) treatments on fruits were performed in a 22 liter glass container. For ethylene treatment on fruit, breaker stage fruits were treated with ethylene gas (50 µl l^{-1}) for 24 h. 1-MCP treatments (1.0 mg l^{-1}) were applied to 3 d post-breaker (turning) fruits for 72 h. Control fruits were incubated in air instead of ethylene or 1-MCP.

Ethylene measurement

Fruits from different developmental stages were harvested and placed in 125 ml jars as previously described (Liu *et al.*, 2014). After 2 h of incubation, 1 ml of headspace gas was injected into an Agilent 7820A gas chromatograph. Quantification was achieved with a flame ionization detector by comparison with ethylene standards.

Firmness measurement

Fifteen fruits from each *Sl-AGL11OE* line and the WT were harvested at different development stages (from DPA10 to BR+10). The firmness was then assessed using Harpenden calipers (British Indicators Ltd) as described by Ecarnot *et al.* (2013).

Water loss

Ten fruits from the WT and three *Sl-AGL11OE* lines were harvested at the breaker stage. Fruits were placed at room temperature for 10 d, and fresh weight was recorded every day. Water loss was calculated as a percentage of fresh weight difference between the starting weight and each individual measurement.

Soluble sugar and starch determination

Fruits and sepals were harvested and frozen in liquid nitrogen. After grinding the fruits into a frozen powder, the samples were incubated with 80% ethanol (10 mM HEPES-KOH pH 7.4) at 80 °C for 15 min, as described by Sonnewald *et al.* (1991). After centrifugation (15 min 16 000 *g*), supernatants were kept for soluble sugar determination: ethanol was removed with a centrifugal vacuum concentrator and, after appropriate dilution in water, glucose, fructose, and sucrose were determined using the Sucrose/Fructose/D-Glucose Assay Kit (Megazyme). For starch, the pellet was rinsed with 80% ethanol (80 °C, 15 min of incubation) and centrifugation. Starch was determined using the Total Starch HK Assay Kit (Megazyme) following the manufacturer's instructions.

Histological observations

To observe fruit anatomy and determine the number of cells layers, fruits were hand-cut and stained using a 30 s bath of 0.05% (w/v) aqueous toluidine blue O (Sigma-Aldrich) followed by two rinses with distilled water. After mounting in water with a cover slip, observations were performed in an Axio Zoom V16 microscope (Zeiss).

To assay defects in synthesis/release of mucilage, dry seeds were hydrated in water for 2 h, stained in 0.03% solution of ruthenium red (Sigma) for 30 min at room temperature, and then rinsed with water. To visualize the seed coat, immature and dry seeds were incubated for 30 min to 1 h in 1% vanillin (Sigma) in 6 M HCl.

For starch visualization, fruit sections were stained in a 0.5× Lugol solution (1% I_2 and 2% KI in water) with a 10 s bath. The excess stain was removed by gently tipping on a paper tissue, and rinsing with distilled water.

RNA-Seq analyses and data processing

Global expression of tomato genes was determined by replicated strand-specific Illumina RNA-Seq. Paired-end RNA sequencing (2 × 150 nucleotdes) was carried out using the Truseq Illumina SBS Kit V4 and the Genotoul Hiseq 2500 platform (http://get.genotoul.fr/). For each line (WT and *Sl-AGL11OE*-L2), RNA was extracted from DPA10 fruits and sepals of three biological replicates. Prior to sequencing, purified RNA quality was checked with the Agilent 2100 Bioanalyzer (rin >8.5).

Raw paired-end RNA-seq sequences in FASTQ format were analyzed as follows. Low quality reads were removed with the FASTQ quality filter using the FASTX toolkit version 0.0.13 (http://hannonlab.cshl.edu/fastx_toolkit/). Trimmed reads were then mapped to the *S. lycopersicum* reference genome and gene annotation (ITAG2.4; Tomato Genome Consortium, 2012) using TopHat-2.0.14 (Trapnell *et al.*, 2009) calling bowtie 2.1.0 (Langmead and Salzberg, 2012).

The differential expression analysis has been carried out with the DESeq2 R package with default settings (Love *et al.*, 2014). The normalization method used by default (LRE) agrees with the assumption that <50% of genes are up-regulated and <50% of genes are down-regulated between two given conditions (Maza *et al.*, 2013;

Maza, 2016). The false discovery rate (FDR) is controlled by the Benjamini–Hochberg method; genes were declared as differentially expressed genes (DEGs) if the adjusted *P*-value was <0.05.

All statistical analyses have been performed with the R software (https://www.r-project.org). The multidimensional scaling analysis (MDS) has been performed with the cmdscale function of the stats R package. This analysis coincides with the principal component analysis (PCA) in the present case where we calculate the Euclidean distance between samples. Expression data were visualized using the MAPMAN 3.5.1 software (Thimm *et al.*, 2004).

Accession numbers

All RNA-Seq data were placed in the European Nucleotide Archive (ERR1904926–ERR1904937).

Results

Sl-AGL11, *a class D MADS-box gene mainly expressed during early fruit development*

Four *AGAMOUS-like* genes—*TAG1* (Solyc02g071730), *TAGL1* (Solyc07g055920), *Sl-AGL11* (Solyc11g028020), and *Sl-MBP3* (Solyc06g064840)—were found in the tomato genome. Based on a phylogenetic analysis (Supplementary Fig. S1) and consistent with previous functional characterization, *TAG1* and *TAGL1* belong to the class C *SHP/Plena* lineage that comprises both the *AGAMOUS* and *SHATTERPROOF* members (Pnueli *et al.*, 1994; Vrebalov *et al.*, 2009). The two other genes, *Sl-AGL11* and *Sl-MBP3*, are highly similar to the petunia *FBP11* and *FBP7* genes and belong to class D function. This D lineage also contains the Arabidopsis *SEEDSTICK* (*STK*, *At4g09960*) gene, which is involved in seed development and seed abscission (Pinyopich *et al.*, 2003). Amino acid sequence comparison indicates that *Sl*-AGL11 and *Sl*-MBP3 share 91% identity, whereas the sequence conservation falls to 56–59% identity when comparing *Sl*-AGL11 with TAGL1 and TAG1.

The expression of *Sl-AGL11* determined by qPCR revealed a clear preferential expression in flower and fruit, especially at early stages of fruit development, and a weak expression in vegetative organs (Fig. 1A). Within the fruit organ, *Sl-AGL11* expression is high in the central part of the fruit, with steady expression levels in the seed and in the 'inner tissues' that comprise the septum, the locular tissue, the placenta, and the columella (Fig. 1C). Moreover, the expression pattern of *Sl-MBP3* seems similar to that of *Sl-AGL11*, as it is also expressed in young fruits with high levels in the seed and the 'inner tissues' (Fig. 1B). These data are in agreement with the expression patterns established *in silico* using the TomExpress database (Zouine et al. 2017; http://gbf.toulouse.inra.fr/tomexpress/) that combines a large number of RNA-Seq expression studies (Supplementary Fig. S2). Interestingly, the four *AGAMOUS-like* genes exhibit their maximum expression level at different developmental stages: *TAG1* reaches its maximum in bud and opened flower, *Sl-AGL11* and *Sl-MBP3* in young fruits, and *TAGL1* at the beginning of ripening (breaker stage), thus suggesting that despite their ancestral origin, the different *AGAMOUS-like* genes have evolved by acquiring temporal-specific expression patterns.

To gain insight into the subcellular localization of *Sl*-AGL11, two different fusion constructs, the C-terminal *35S-Sl-AGL11-GFP* and the N-terminal *35S-YFP-Sl-AGL11*, were transiently expressed in tobacco BY-2 protoplasts. For both constructs, the fluorescence signals were found mainly in the nucleus but also extended to the cytoplasmic compartment (Supplementary Fig. S3). Considering the putative function of *Sl*-AGL11 as a transcription factor, these data suggest that it might undergo important regulation at the post-translational level.

Sl-AGL11 *down-regulation results in a limited effect on seeds*

To investigate the functional significance of *Sl-AGL11*, we generated 12 independent tomato transgenic lines exhibiting down-regulation of the *Sl-AGL11* gene through an RNAi approach designed to target specifically this class D member. Transcript level analysis performed by qPCR on young fruits (DPA10 stage) confirmed that *Sl-AGL11* was substantially down-regulated whereas *Sl-MBP3*, its closest class D homolog, remained unaffected (Fig. 2B). Out of the 12 RNAi lines generated, none exhibited visually detectable phenotypes, either in the vegetative organs or in the fruits, where *Sl-AGL11* is normally expressed (Fig. 2A, C). Despite a 60–77% decrease of *Sl-AGL11* expression, which was confirmed by qPCR for nine RNAi lines (Supplementary Fig. S4), all transgenic lines produced seeded fruits, in contrast to previous reports also using an RNAi strategy (Ocarez and Mejía, 2016). Nonetheless, a slight decrease in seed size and an average 20% reduction of seed weight were observed (Fig. 2C). Also, ruthenium red or vanillin staining of seeds did not reveal any change in mucilage and flavonoid accumulation in the seed coat (Supplementary Fig. S5).

Sl-AGL11 *overexpression induces dramatic modifications in flower and fruit organization*

Since the phenotypes due to *Sl-AGL11* down-regulation were visually subtle and apparently restricted to seed, we generated tomato plants overexpressing the *Sl-AGL11* coding sequence under the control of the 35S promoter in order to gain further insight into the putative function of this tomato class D member. Fifteen independent transgenic lines, named *Sl-AGL11OE*, were generated, and all displayed dramatic phenotypes associated with flower and fruit development (Fig. 3A).

In all these lines, the expression of *TAG1*, *TAGL1*, and *Sl-MBP3* assessed at the transcript level showed no significant alteration, with the exception of *TAGL1* which displayed a slight decrease in transcript accumulation in one of the *Sl-AGL11OE* lines (Supplementary Fig. S6). No major alteration of vegetative development was observed except a minor reduction in plant size in some lines only visible in adult plants since young plants were unaffected (Fig. 3A; Supplementary Fig. S7). In contrast, *Sl-AGL11OE* plants demonstrated severe phenotypes visible at early flower bud stages with defects in sepal development. The sepals were light green, swollen, and

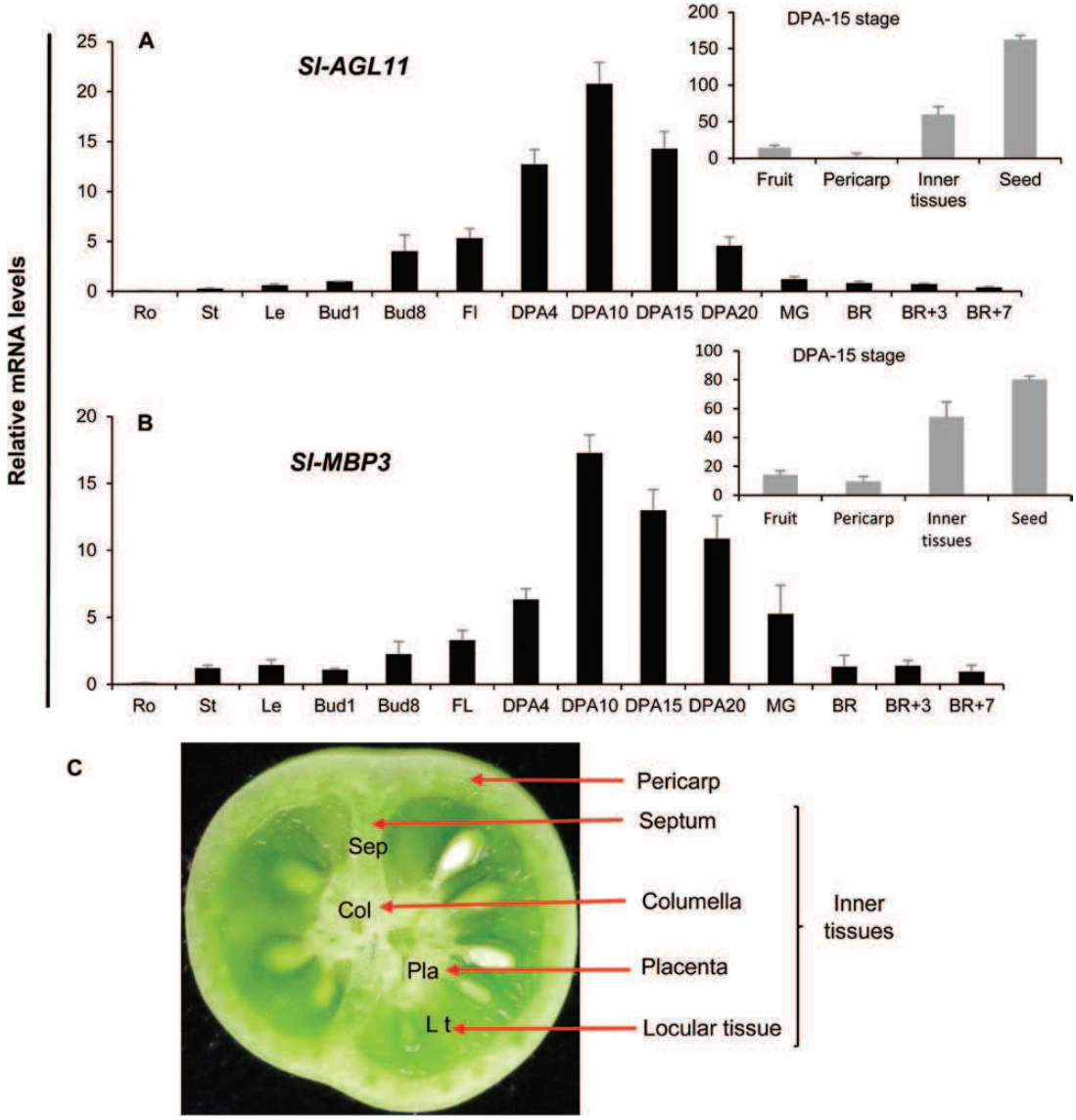

Fig. 1. Expression pattern of *Sl-AGL11*. (A) *Sl-AGL11* expression in different tissues determined by qPCR. Ro, root; St, stem; Le, leaf; Bud1, Bud8, 1 mm and 8 mm long flower buds; Fl, opened flower at anthesis; DPA4, DPA10, DPA15, DPA20, fruit at 4, 10, 15 and 20 d, respectively, after anthesis; MG, mature green fruit; BR, fruit at breaker stage; BR+3, BR+7: fruits 3 d and 7 d after the BR stage. Values are means ± SD of three biological replicates. (B) *Sl-AGL11* expression in different DPA15 fruit tissues. 'Inner tissues' comprise columella, placenta, septum, and locular tissue. Values are means ± SD of three biological replicates. (C) 'Inner tissues' in young tomato section including columella, septum, placenta, and locular tissue.

failed to open at anthesis (Fig. 3A). In the most severe lines, the sepals virtually enclosed the ovary, thus preventing pollen dispersion and leading to the development of seedless fruit (Supplementary Fig. S8). Three lines exhibiting a 20- to 30-fold increase in *Sl-AGL11* transcript level (Fig. 3B) were selected for further characterization. In the *Sl-AGL11OE* lines, as the fruit entered the ripening process, the sepals evolved like a fleshy fruit, turning orange and then red, suggesting that they differentiated into a succulent organ that shared most fruit attributes. Besides sepals, the flower peduncles in *Sl-AGL11OE* plants were nearly glabrous with few trichomes, and underwent swelling and ripening (Supplementary Fig. S9). In contrast to the sepal, no major difference was observed in petal structure (Fig. 3A). Another remarkable feature of the *Sl-AGL11OE* plants is the lack of an activated abscission zone at the middle of the pedicel which prevents the fruit from dropping from the plant at the end of the ripening process (Supplementary Fig. S9). Fruit development was also dramatically affected in *Sl-AGL11OE* plants, with reduced fruit size and weight (Supplementary Fig. S10A). Histological observations on fruit sections stained with toluidine blue revealed dramatic modifications in both pericarp and inner tissues, including gel, placenta, and columella. The fruit size was reduced and the pericarp was typically thinner in *Sl-AGL11OE* fruits, with smaller cells even though the number of cell layers was slightly higher (Supplementary Fig. S10B). In the inner part of the *Sl-AGL11OE* fruits, we observed a marked reduction of the locular space that was restricted to a thin 'jelly' surrounding the seeds (Fig. 3C), while the relative area corresponding to the placenta was increased (Fig. 3D). Moreover, *Sl-AGL11OE* lines did not exhibit any delay in flowering initiation (Supplementary Fig, S11). The fruits of *Sl-AGL11OE* lines produced few or no

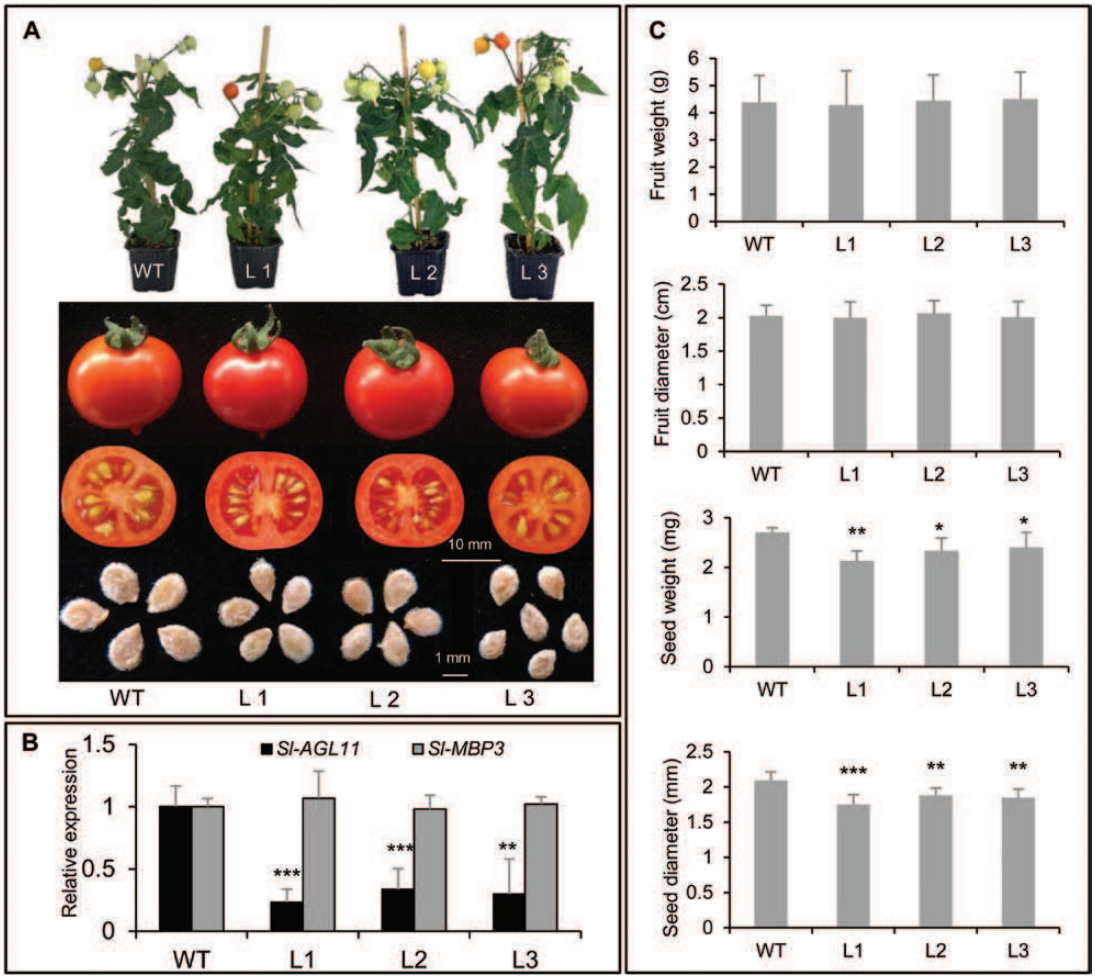

Fig. 2. Phenotype of tomato lines with RNAi-mediated down-regulation of *Sl-AGL11*. (A) Observation of plants, fruits, and seeds in three representative independent lines. (B) Relative down-regulation level of *Sl-AGL11* monitored by qPCR on young fruits (DPA10 stage). Values are means ±SD of three biological replicates. (C) Quantification of mean weight and size of fruits (n=15) and seeds (n=120) in three representative independent lines compared with the wild type (WT). Values are means ±SD. Statistical significance determined by Student's t-test: *0.01<P<0.05; **0.001<P<0.01; ***P<0.001. L1–L3 are three independent *Sl-AGL11*-RNAi lines. (This figure is available in colour at *JXB* online.)

seeds. However, manual flower cross-pollination with WT pollen restored almost normal seed development (Supplementary Fig. S12). Cross-fertilization of emasculated WT flowers could not restore normal seed development, revealing pollen deficiency in *Sl-AGL11OE* plants (Supplementary Fig. S12). Therefore, the selected transgenic lines were maintained and multiplied as hemizygous lines by cross-pollination with WT pollen and subsequent antibiotic selection of seedlings.

Sl-AGL11OE *fruits and sepals undergo a ripening-like process that is ethylene dependent*

Since *Sl-AGL11OE* fruit development was altered and plant sepals differentiated into fleshy tissues, we examined the ripening dynamics of *Sl-AGL11OE* fruit and fleshy sepals. Compared with WT fruit, color change in *Sl-AGL11OE* occurs more slowly, suggesting a delay in the onset of ripening (Fig. 4A). Accordingly, the peak of climacteric ethylene was delayed by 5–6 d in *Sl-AGL11OE* fruits while the amount of ethylene produced was enhanced 3-fold (Fig. 4B). In addition, exogenous ethylene treatment proved to be efficient in inducing ripening and, conversely, treatment with 1-MCP, an inhibitor of ethylene perception, prevented ripening, thus confirming that fruit and succulent sepals in *Sl-AGL11OE* plants behave as climacteric organs (Fig. 4C). We then examined the expression of a set of key ripening genes including the ethylene synthesis genes ACC *oxidase1* (*ACO1*) and ACC *synthase2* (*ACS2*), as well as two major regulators of climacteric ripening *Ripening Inhibitor* (*RIN*) and *Non-Ripening* (*NOR*) genes. For all four ripening-associated genes, the expression level increased during ripening until the BR+7 stage, where it was significantly higher than in WT fruits (Fig. 4D), fully consistent with the pattern of ethylene production.

Sl-AGL11 *overexpression has dramatic effect on fruit firmness*

In addition to the acquisition of fleshy sepals, another remarkable feature displayed by the *Sl-AGL11OE* fruit consists of a dramatic decrease in firmness starting at an early stage of fruit development well before ripening (Fig. 5A). When they reach the ripening stage, the fruits become difficult to handle

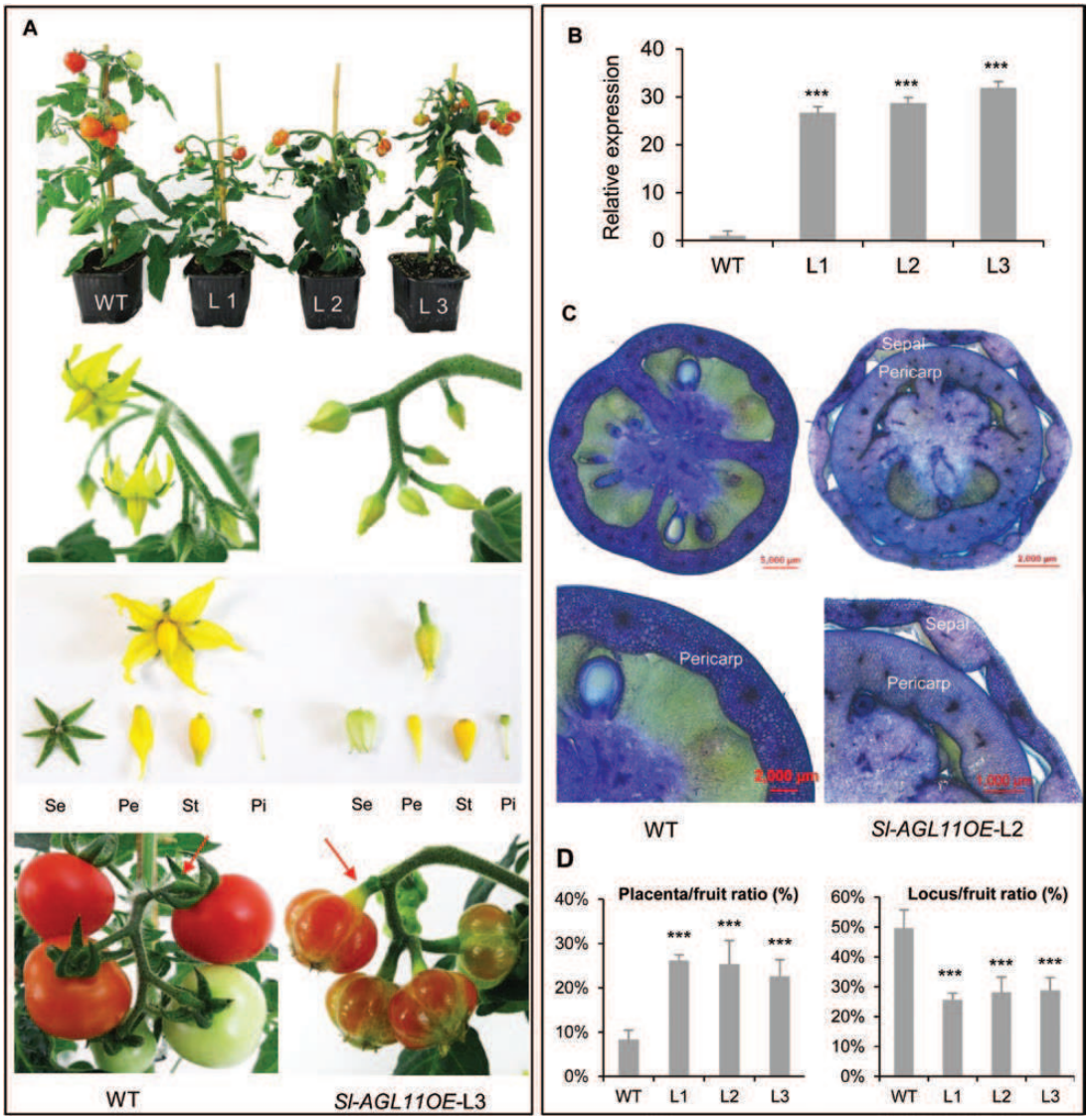

Fig. 3. Dramatic modifications in flower and fruit organization triggered by 35S-driven *Sl-AGL11* overexpression. (A) Flower and fruit morphology of wild-type (WT) and *Sl-AGL11OE* (L3). Se, sepal; Pe, petal; St, stamen; Pi, pistil. (B) Transgene expression level in three *Sl-AGL11OE* lines monitored by qPCR using DPA10 fruits tissue. Values are means ± SD of three biological replicates. (C) Histological observations of fruit and sepal in WT and *Sl-AGL11OE* (L2) at the DPA20 stage. Sections were stained with toluidine blue. (D) Relative proportions of inner tissues of tomato fruits at the ripening stage for WT and *Sl-AGL11OE* lines deduced from the area ratios. A total of 15 fruits was used for each line measurement. Values are means ± SD. Asterisks indicate statistical significance using Student's *t*-test: ***P<0.001. L1–L3 are three independent *Sl-AGL11OE* lines. (This figure is available in colour at *JXB* online.)

and often burst upon manipulation. Measurement of firmness by Harpenden calipers (Fig. 5B) confirmed that this loss of firmness occurred very early during fruit development. In addition to the enhanced softness, other modifications may affect the cuticle as upon harvest the *Sl-AGL11OE* fruits display accelerated water loss compared with control WT fruits (see Supplementary Fig. S13). We therefore monitored the expression of four cell wall-related genes known to be involved in ripening-associated cell wall modifications: polygalacturonase *PG2A* (Grierson *et al.*, 1986), β-galactosidase *β-GAL4* (Smith *et al.*, 2002), expansin *EXP1* (Brummell *et al.*, 1999), and pectate lyase *PL2* (Uluisik *et al.*, 2016). We also monitored three additional genes whose expression was highly affected in the '*Sl-AGL11OE*-fruit' versus 'WT-fruit' RNA-Seq experiment described below: xyloglucan-endosyltransferase *XTH1* (Solyc01g099630), pectin acetyl transferase *PAE-like* (Solyc08g005800), and cellulose synthase *CS-like* (Solyc07g051820). In agreement with the RNA-Seq data, the expression of the four cell wall-related genes more commonly associated with ripening (*EXP1*, *PG2A*, *β-GAL4*, and *PL2*) showed no major difference between WT and *Sl-AGL11OE* fruits at DPA10 and their transcript levels showed an increase only at the onset of fruit ripening (Fig. 5C). In contrast, *XTH1*, *PAE-like*, and *CS-like* expression was dramatically reduced in *Sl-AGL11OE* fruit samples (Fig. 5C), suggesting that the enhanced softness exhibited by *Sl-AGL11OE* fruits may originate from early modifications in fruit cell wall differentiation.

Sl-AGL11-*overexpressing fruit accumulate more sugar*

Preliminary observations based on the staining of *Sl-AGL11OE* fruits with iodine suggested important

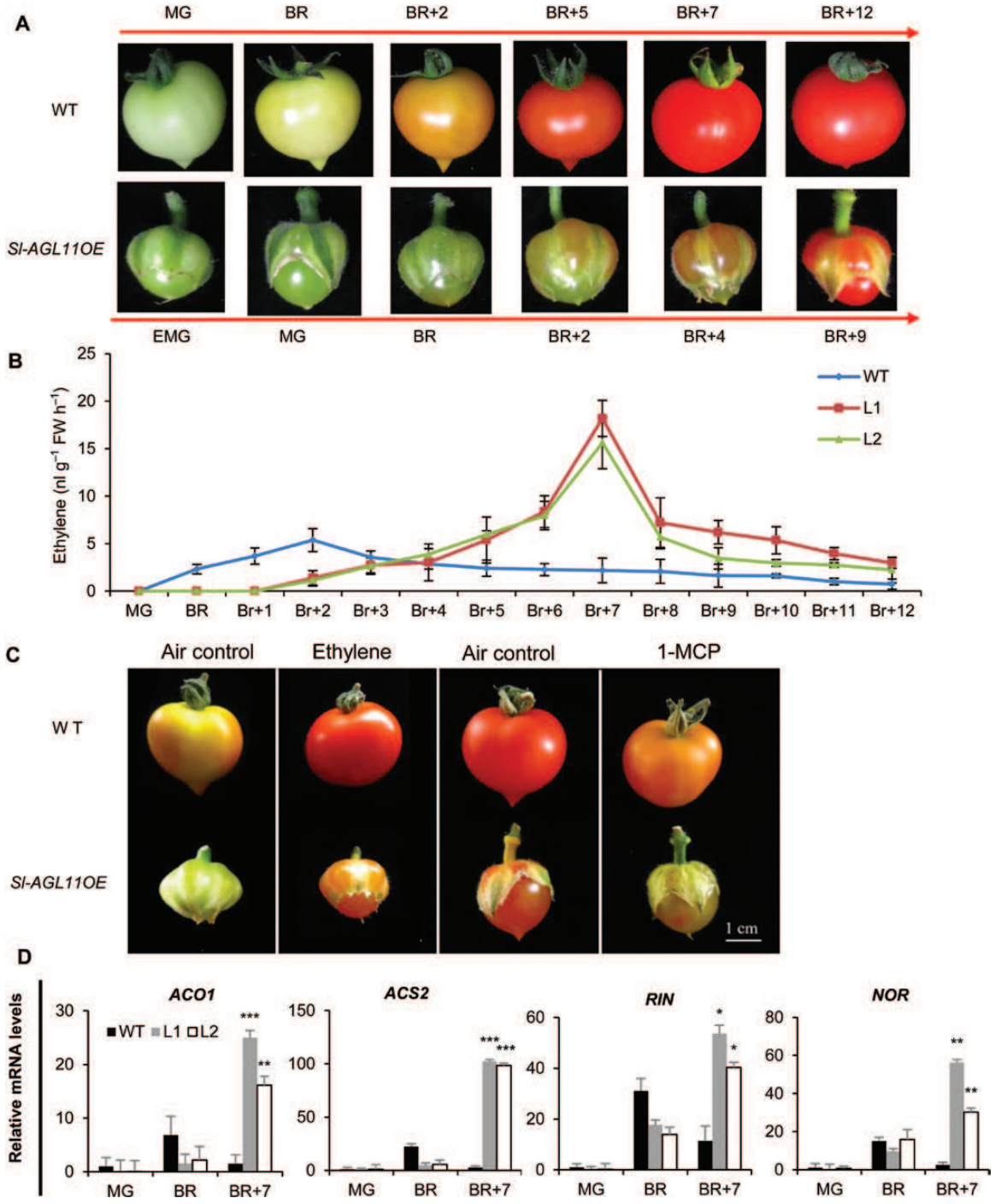

Fig. 4. Ripening characteristics of *Sl-AGL11*-overexpressing fruits and sepals. (A) Color changes associated with ripening in wild-type (WT) and *Sl-AGL11OE* fruits and sepals. For the two genotypes, the breaker stage was defined as the onset of the color change. EMG, early mature green; MG, mature green; BR, breaker; BR+2, BR+4, BR+5, BR+7, BR+9, BR+12, days post-breaker. (B) Ethylene production associated with fruit ripening in WT and *Sl-AGL11OE* fruits (n=15 fruits); values are means ± SD. (C) Effect of exogenous ethylene and 1-MCP treatment on fruit ripening. Ethylene treatment (and air control) were applied at the breaker stage. 1-MCP (and air control) were applied at BR+3 (turning) stage. (D) Evolution of the expression of four ripening-related genes (*AOC1*, *ACS2*, *RIN*, and *NOR*) assessed by qPCR. Error bars are the mean ± SD of three biological replicates. Asterisks indicate statistical significance using Student's t-test: *$0.01<P<0.05$;**$0.001<P<0.01$; *** $P<0.001$. L1 and L2 are two independent *Sl-AGL11OE* lines. (This figure is available in colour at *JXB* online.)

modifications in starch and sugar accumulation (Fig. 6A). Monitoring starch evolution in fruits confirmed a 2-fold increase in *Sl-AGL11OE* green tomatoes and revealed that starch breakdown was delayed (Fig. 6A, B). Soluble sugars were then quantified in ripening fruits. In ripe fruit (BR+12 stage), glucose and fructose were higher in *Sl-AGL11OE* fruits, with a 1.5- and 2-fold increase, respectively (Fig. 6C). Notably, while sucrose was found at trace levels in WT fruits, its concentration reached up to 28 g kg^{-1} at the late ripening stages (BR+12) in *Sl-AGL11OE* fruits (Fig. 6C). Sepals of *Sl-AGL11OE* plants also contained high concentrations of starch and soluble sugars, further confirming that the

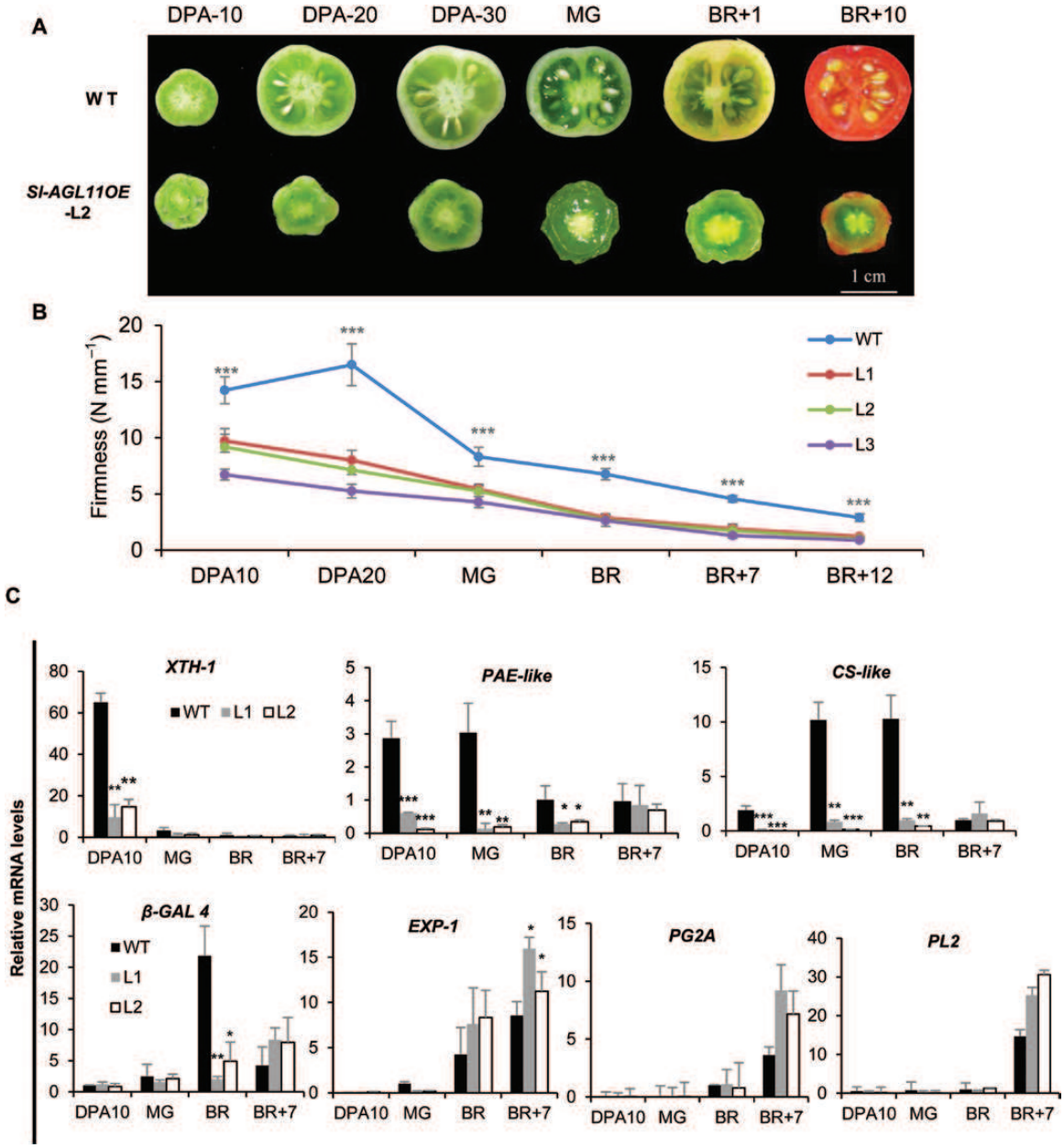

Fig. 5. Dramatic effect of *Sl-AGL11* overexpression on fruit firmness. (A) Morphology of *Sl-AGL11OE* (L2) and wild-type (WT) fruit during development and ripening. DPA10, DPA20, DPA30, fruit at 10, 20, and 30 d after anthesis, respectively; MG, mature green; BR+1, BR+10, days post-breaker. (B) Evolution of fruit firmness during fruit development and ripening. A *t*-test was performed between the wild type (WT) and each individual *Sl-AGL11OE* line (n=15 fruits per stage); values are means ± SD (***P-value <0.001). (C) Evolution of the expression level of softness-related genes in fruit development and ripening assessed by qPCR. *XTH-1*, Solyc01g099630; *PAE-like*, Solyc08g005800; *CS-like*, Solyc07g051820; *PG2A*, Solyc10g080210; β-*GAL4*, Solyc12g008840; *EXP-1*, Solyc06g051800; *PL2*, Solyc03g111690.Values are means ± SD of three biological replicates. Significance was determined by Student's *t*-test: *0.01<P<0.05; **0.001<P<0.01; *** P<0.001. L1–L3 are three independent *Sl-AGL11OE* lines. (This figure is available in colour at *JXB* online.)

conversion into a fleshy organ implies similar metabolic reorientations to those occurring in genuine fruit tissues (Fig. 6C).

Genome-wide transcriptomic profiling of Sl-AGL11OE *fruit and sepals*

As the major histological and physiological changes in *Sl-AGL11OE* lines were observed during early fruit development, we performed a global gene expression profiling of young fruits and sepals harvested at the DPA10 stage. The RNA-Seq analysis produced, after removing the low quality reads, ~325 million paired-end reads, with a total number of reads for each sample ranging from 16 million to 39 million. On average, 83% of these reads were mapped to the ITAG-2.4 tomato reference genome, producing 13.5–30 million unique mapping reads depending on the sample considered. The number of predicted genes covered with a minimal average density of 20 independent counts per kilobase was ~60% (Supplementary Data S1). DEGs between various samples and conditions were identified with the following rules: mean

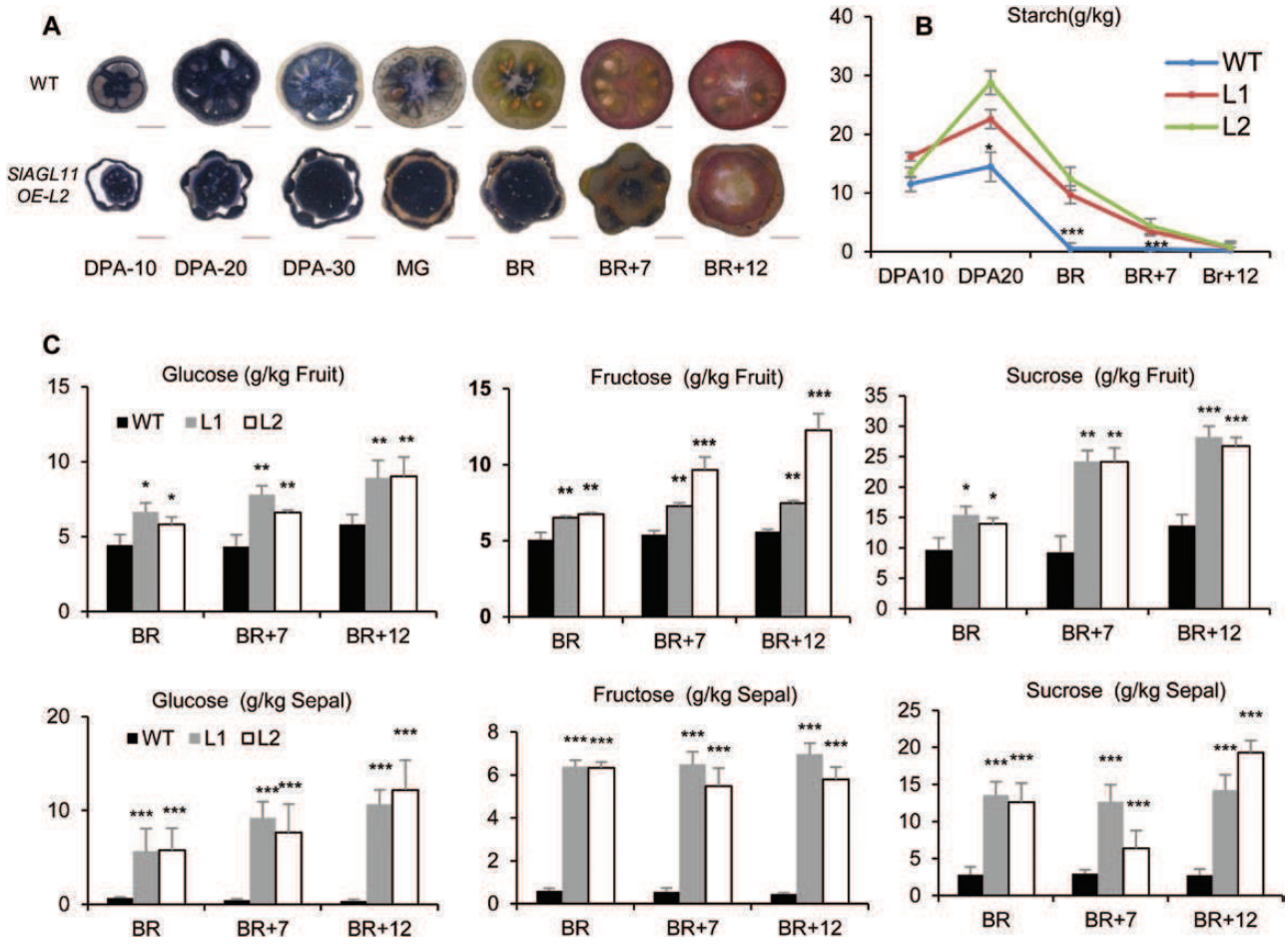

Fig. 6. Evolution of starch and soluble sugars during development and ripening of *Sl-AGL11*-overexpressing fruit. (A) Iodine coloration of wild-type (WT) and *Sl-AGL11OE* (L2) fruits at different stages. DPA10, DPA20, DPA30, fruit at 10, 20, and 30 d after anthesis, respectively; MG, mature green; BR, breaker; BR+7, BR+12, days post-breaker. Scale bars=500 μm. (B) Evolution of fruit starch content at different development stages (n=6 fruits per stage); values are means ± SD, a *t*-test was performed between WT and each individual *Sl-AGL11OE* line. *0.01<*P*<0.05; ***P*<0.001. (C) Evolution of soluble sugar contents during ripening measured with glucose, fructose, and sucrose concentrations. Values are means ± SD of six biological replicates. Statistical significance was determined by Student's *t*-test: *0.01<*P*<0.05; **0.001<*P*<0.01; *** *P*<0.001. L1 and L2 are two independent *Sl-AGL11OE* lines. ruit at 10, 20, and 30 d after anthesis, respectively. (This figure is available in colour at *JXB* online.)

normalized counts kb^{-1} >20 and adjusted *P*-value <0.05 (Supplemental Data S2, S3).

Performing a PCA on normalized mRNA-Seq counts confirmed that the biological replicates clustered together in both the sepal and the fruit (Fig. 7A). More interestingly, the same PCA analysis revealed that the first axis, holding 70% of the variability, could only separate WT sepals, *Sl-AGL11OE* sepals, and a cluster comprising both WT and *Sl-AGL11OE* fruits. Yet, the fruit samples were clearly discriminated through the second and following axes. Conversely, among the genes that displayed differential expression in the WT fruit versus WT sepal (12 389), more than half (6355) were also differentially expressed in the *Sl-AGL11OE* succulent sepals versus WT sepals experiment (Fig. 7B). Based on this preliminary analysis, the position of *Sl-AGL11OE* sepals along the first axis already suggests that the conversion of sepals into a succulent organ creates a kind of intermediary organ between a vegetative sepal and a fleshy fruit.

In order to identify specific functions impacted by the over-expression of *Sl-AGL11*, DEGs were associated with their respective MAPMAN gene annotation category (Thimm *et al.*, 2004). The functional categories displaying the highest over-representation were determined using a Wilcoxon rank sum test on the MAPMAN bins for the *Sl-AGL11OE* versus WT fruit and *Sl-AGL11OE* versus WT sepal experiments (Fig. 7C). When comparing WT and *Sl-AGL11OE* sepals or fruit, 'Photosynthesis', 'RNA processing', and 'Cell wall' categories were over-represented for both tissues (Fig. 7C). Consistent with the transition from a green sepal to a fleshy ripening organ, the complete set of photosynthesis-related genes is repressed in *Sl-AGL11OE* lines (Supplementary Fig. S14).

Since *Sl-AGL11OE* plants exhibited a marked softness and a different pattern of toluidine blue staining (Figs 3C, 5A), a dye known for its metachromatic properties, we focused our analyses on the expression of different cell wall genes. Out of the 306 annotated cell wall genes expressed in fruit, 134 genes (44%) were differentially expressed in the *Sl-AGL11OE* versus WT DPA10 fruit experiment. Strikingly, 82% of these DEGs were down-regulated (Supplementary Data S2); this proportion reached 90% when considering only DEGs with high expression and a marked difference ($|\log_2 fold|>1$, Table 1).

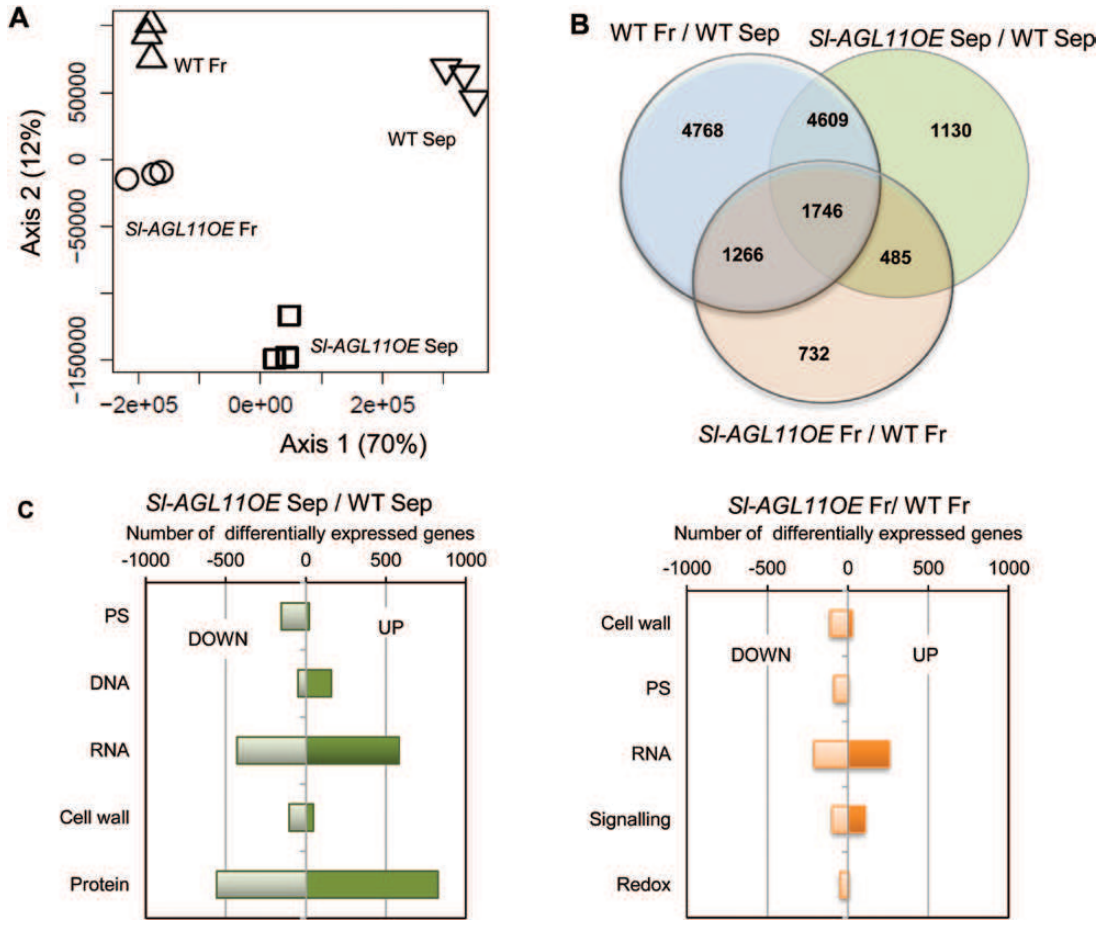

Fig. 7. RNA-Seq expression profiling of tomato young fruits and sepals overexpressing *Sl-AGL11*. (A) Principal component analysis based on all expressed genes. The projection of axes 1 and 2 that held 82% of the inertia showed four distinct groups of experiments. (B) Distribution of DEGs in the different experiments as illustrated by a Venn diagram using the following rule: *n*(counts kb^{-1}) >20; adjusted *P*-value <0.05. (C) Categories enriched in the (*Sl-AGL11OE* versus the WT) sepal and (*Sl-AGL11OE* versus WT) fruit experiments. Only the five categories with the highest *P*-values are shown. PS, photosynthesis (light reaction, photorespiration, Calvin cycle); DNA, DNA synthesis, chromatin structure, DNA repair; RNA, RNA processing, transcription process, transcription regulation (including transcription factors), RNA-binding proteins; Cell wall, synthesis, modification, and degradation of different cell wall components (precursors, cellulose, hemicellulose, pectins, HGRP); Protein, translation, targeting, post-translational modifications, folding, degradation, assembly; Signaling, receptor-kinases, MAP-kinases, calcium, phosphoinositides, G-protein transduction pathways, light- and nutrient-related signaling pathways; Redox, thioredoxins, heme-proteins, ascorbate and glutathione metabolism, glutaredoxins, peroxiredoxins, dismutase, catalase. Fr, fruit; Sep, sepal. (This figure is available in colour at *JXB* online.)

Interestingly, several cell wall genes whose homologs are targets of Arabidopsis *STK*, such as cellulose synthase *CESA5* and *CESA2*, cellulose synthase-like *CSLA2*, and *COBRA-LIKE 2 COBL2* (Ezquer *et al.*, 2016), were down-regulated in *Sl-AGL11OE* fruits (Supplementary Table S1).

Discussion

In tomato, the C/D lineage of *AGAMOUS*-related genes consists of four paralog genes: *TAG1*, *TAGL1*, *Sl-AGL11*, and *Sl-MBP3*. Various expression studies collected in the TomExpress database (Supplementary Fig. S2) have shown that the four *AGAMOUS* paralogs in tomato display temporal-specific expression patterns, with the class D genes *Sl-AGL11* and *Sl-MBP3* being preferentially expressed in early fruit development. Expression studies confirmed the high transcript levels of *Sl-AGL11* and *Sl-MBP3* in developing flowers and young fruits, reaching a maximum value in the inner part of young fruits that comprises placenta, seed, and columella (Fig. 1C). A laser-assisted microdissection on young *Solanum pimpellifolium* fruits (Pattison *et al.*, 2015) revealed similar expression patterns for the two class D isoforms (*Sp-AGL11* and *Sp-MBP3*) as they are both found in seed and inner fruit tissues (seed coat, endosperm, funiculus, embryo, placenta, and septum). This contrasts with petunia dry fruit, where the expression of *FBP11* and *FBP7* class D genes was restricted to seeds and ovule (Colombo *et al.*, 1997). Thus, the expression pattern observed in tomato suggests an additional role for *Sl-AGL11* or *Sl-MBP3* that extends beyond seed development.

The initial approach consisting of *Sl-AGL11* down-regulation resulted in a subtle phenotype affecting seed size, in agreement with class D function defined as regulating ovule and seed development. However, our data clearly contrast with a previous report (Ocarez and Mejía, 2016) stating that *Sl-AGL11* down-regulation leads to seedless tomato fruits. Moreover the seedlessness phenotype reported by Ocarez and

Table 1. *List of cell wall-related genes differentially expressed in* SI-AGL11OE *fruit*

DEGs were deduced from the DPA10 fruit *SI-AGL11OE* versus WT RNA-Seq experiment using the following rule: *n*(counts kb^{-1}) >20; $|\log_2 fold|>1$ and *P*-value <0.05.

MAPMAN category	Solyc number	Log_2 fold	Description
10.1: Precursor synthesis (26/56/68)[a]	Solyc08g080570	1.1	UDP-glucose 4-epimerase
	Solyc07g014640	–1.1	Galactokinase-like protein
	Solyc08g080140	–1.2	dTDP-4-dehydrorhamnose reductase
	Solyc07g006220	–1.3	UDP-D-glucuronate 4-epimerase 1
	Solyc09g092330	–1.5	NAD epimerase/dehydratase.
	Solyc02g084210	–1.7	GDP-mannose 4 6-dehydratase
	Solyc03g096730	–2.4	GDP-D-mannose pyrophosphorylase 1
10.2: Cellulose synthesis (8/24/86)[a]	Solyc04g071650	–1.1	Cellulose synthase
	Solyc11g066820	–1.2	Cellulose synthase-like C6
	Solyc09g008990	–1.5	Cellulose synthase-like A2
	Solyc09g009010	–1.6	Cellulose synthase-like C1
	Solyc06g074630	–1.6	Cellulose synthase-like C6
	Solyc10g083670	–2	Cellulose synthase-like C2
	Solyc12g014430	–2	Cellulose synthase
	Solyc07g051820	–6.2	Cellulose synthase
10.5: Cell wall proteins (15/33/50)[a]	Solyc03g114860	–1.1	Alpha-1 4-glucan-protein synthase
	Solyc03g019750	–2.2	Alpha-1 4-glucan-protein synthase
	Solyc10g054900	–2.4	Proline-rich protein
	Solyc07g053540	–3.3	Fasciclin-like arabinogalactan protein 4
10.6: Cell wall degradation (36/89/181)[a]	Solyc09g075360	1.6	Endoglucanase 1
	Solyc03g058910	1.1	Pectate lyase
	Solyc06g073760	1.1	Beta-D-glucosidase
	Solyc07g049300	–1.1	Polygalacturonase
	Solyc01g110340	–1.1	BURP domain-containing protein
	Solyc03g116500	–1.2	Pectate lyase
	Solyc08g068150	–1.3	BURP domain-containing protein
	Solyc06g083580	–1.3	Pectate lyase
	Solyc02g084990	–1.4	Polygalacturonase
	Solyc05g005080	–1.5	BURP domain-containing protein
	Solyc05g005560	–1.5	BURP domain-containing protein
	Solyc04g081300	–1.5	BURP domain-containing protein
	Solyc08g082250	–1.5	BURP domain-containing protein
	Solyc05g014000	–1.5	Mannan endo-1 4-beta-mannosidase
	Solyc07g064870	–1.6	Mannan endo-1 4-beta-mannosidase
	Solyc04g008230	–1.6	Mannan endo-1 4-beta-mannosidase
	Solyc05g005570	–1.7	Alpha-L-arabinofuranosidase/beta-D-xylosidase
	Solyc10g008300	–1.7	Endo-1 4-beta-xylanase
	Solyc06g064520	–1.7	Mannan endo-1 4-beta-mannosidase
	Solyc04g072850	–2.2	Endoglucanase 1
	Solyc05g051260	–2.3	Endoglucanase 1
	Solyc01g109500	–2.4	Endo-1 4-beta-glucanase
	Solyc05g005550	–4.5	Endoglucanase 1
	Solyc01g008720	–6.6	Endoglucanase 1
	Solyc05g052530	–7.2	Endoglucanase 1
	Solyc02g062320	–7.9	Endoglucanase 1
10.7: Cell wall modification (17/35/81)[a]	Solyc06g051800	1.8	Expansin
	Solyc06g060970	1.2	Expansin
	Solyc07g054170	–1.1	Expansin B1
	Solyc09g010860	–1.6	Expansin
	Solyc07g009380	–2.3	Xyloglucan endotransglucosylase 5
	Solyc01g099630	–2.4	Xyloglucan endotransglucosylase 1
	Solyc02g091920	–3.1	Xyloglucan endotransglucosylase 2
	Solyc09g008320	–3.2	Xyloglucan endotransglucosylase 12
	Solyc03g115310	–3.6	Expansin
	Solyc07g049540	–6.8	Expansin B5
	Solyc11g017450	–8.4	Xyloglucan endotransglucosylase

Table 1. *Continued*

MAPMAN category	Solyc number	Log_2 fold	Description
10.8.1: Phosphomethylesterase (8/24/86)[a]	Solyc03g083360	–1.5	Pectinesterase
	Solyc03g123630	–1.5	Pectinesterase
	Solyc07g017600	–2.2	Pectinesterase
	Solyc12g098340	–2.3	Pectinesterase
	Solyc06g009190	–4.2	Pectinesterase
	Solyc09g091730	–4.5	Pectinesterase
10.8.2: Phosphoacetylesterase (3/6/17)[a]	Solyc08g075020	–1.3	Pectinacetylesterase
	Solyc08g005800	–5.6	Pectinacetylesterase-like

[a]Number of genes in each subcategory, DEGs in *Sl-AGL11OE* versus WT fruits/total expressed genes in fruit/total genes in tomato genome.

Mejía (2016) was based on the analysis of primary transformants (T0 lines) and these authors did not check whether their RNAi strategy affected the second member of the class D clade (*Sl-MBP3*) whose nucleic acid sequence shares 85% identity with *Sl-AGL11*. The absence of a strong seed phenotype in our down-regulated lines is consistent with the data reported in petunia, where a single knockout of class D *FBP7* or *FBP11* did not result in a seedless phenotype whereas major seed defects were visible with simultaneous *FBP7*/*FBP11* down-regulation (Angenent *et al.*, 1995; Colombo *et al.*, 1997; Heijmans *et al.*, 2012). Such redundancies were also reported in Arabidopsis (Pinyopich *et al.*, 2003) and rice (Dreni *et al.*, 2011). In Arabidopsis, redundant activities in the promotion of ovule identity were suggested since ovule and seed development were only abolished in the triple *stk*/*shp1*/*shp2* mutant (Pinyopich *et al.*, 2003). Altogether, these data suggest a partial redundancy among class D genes that varies among plant species, which is consistent with the similar expression pattern of *Sl-AGL11* and *Sl-MBP3* in young developing fruits.

In contrast to the down-regulated lines, *Sl-AGL11*-overexpressing lines exhibited dramatic flower and fruit modifications, notably sepal swelling and conversion into a fleshy organ that eventually underwent a typical ripening process. Our transcriptome analyses highlighted the extent of sepal reprogramming and confirmed that the ectopic expression of *Sl-AGL11* is the causal element as other *AGAMOUS* genes remained almost unaffected. The sepal conversion into a succulent organ is reminiscent of different phenotypes obtained with ectopic expression of different class C *AGAMOUS* genes in tomato such as *TAG1* (Pnueli *et al.*, 1994), *TAGL1* (Itkin *et al.*, 2009; Vrebalov *et al.*, 2009; Giménez *et al.*, 2010), peach *Plena* (Tadiello *et al.*, 2009), grape *VviAGL11* (Mellway and Lund, 2013), and the *Ginkgo biloba GBM5* gene (Lovisetto *et al.*, 2015). In all these studies, the sepal identity modification is often interpreted as a partial conservation of the class C function, similarly to the conversion of sepal to carpelloid structure in Arabidopsis (Mizukami and Ma, 1992), tobacco (Kempin *et al.*, 1993), or *p*etunia (Van Der Krol and Chua, 1993; Kater *et al.*, 1998). Yet, our data support the idea that the C function of *Sl-AGL11* is still incomplete. This is consistent with the absence of petal modifications, in contrast to tomato lines overexpressing class C *TAG1* and *TAGL1* MADS-box genes (Pnueli *et al.*, 1994; Vrebalov *et al.*, 2009). Likewise, no flowering delay occurred, in contrast to Arabidopsis plants overexpressing *AGAMOUS* or *STK* that exhibited mild early flowering (Mizukami and Ma, 1997; Favaro *et al.*, 2003). It is also important to highlight the differences between *Sl-AGL11OE* tomatoes and petunia or Arabidopsis plants overexpressing *FBP11* or *STK* class D genes, respectively (Colombo *et al.*, 1995; Favaro *et al.*, 2003). Indeed, no ovule-like structures were found on the *Sl-AGL11OE* sepals, whereas the ectopic expression of class D genes in petunia and Arabidopsis resulted in a failure to form any carpelloid organ structure. These differences may be interpreted as the consequence of the 'fleshy' background found in tomato. Moreover, the conversion of sepals into fleshy organs suggests that *Sl-AGL11* acts as a class C/D MADS-box gene.

Since *Sl-AGL11* overexpression phenotypes suggested only a partial conservation of class C function, analyzing the similarities and differences between *Sl-AGL11OE* plants and *TAG1*- or *TAGL1*-overexpressing plants should provide leads to uncovering a specific signature of *Sl-AGL11* action. The comparison of *Sl-AGL11OE* phenotypes with those reported in *TAGL1* experiments (Itkin *et al.*, 2009) reveals similar dynamics of sepal conversion. That is, swelling starts at the basis of the calyx in the intersepal tissue and ripening of *Sl-AGL11OE* fruits and sepals matches that of *TAGL1*-overexpressing fruits. Regarding sugar metabolism, the data on *Sl-AGL11OE* plants converge with those reported for *TAGL1*-overexpressing tomatoes which indicated an increase in Brix (Giménez *et al.*, 2010). The enhanced starch phenotype is also consistent with *TAGL1* RNAi experiments reporting a depletion of starch in the pericarp of immature fruits (Vrebalov *et al.*, 2009). In contrast, two features seem specific to *Sl-AGL11* overexpression and may be considered as a distinctive signature: placenta and columella hypertrophy and the extreme softening at the early stage of fruit development. Regarding columella and placenta hypertrophy, it is important to mention that these tissues represent high *Sl-AGL11* expression domains (Fig. 1A). While this may suggest that class D MADS-box genes control the differentiation of the inner tissues of tomato fruits, the biological significance of this signature must be interpreted cautiously since ectopic expression of MADS-box genes can act either by triggering abnormal signaling pathways in tissues where *Sl-AGL11* is normally absent or by creating competition with endogenous MADS-box factors within the tetrameric complex or during

import in the nucleus (Smaczniak *et al.*, 2012; Dreni and Kater, 2014).

The extreme softening of *Sl-AGL11OE* fruits and the different histological staining reflect major cell wall modifications. Analyzing the RNA-Seq data by the MAPMAN annotation tool identified the functional 'Cell wall' category as being clearly enriched in the '*Sl-AGL11OE* versus WT fruit' experiment. Cell wall modifications have been largely studied in ripening-associated softening (Seymour *et al.*, 2013). Among the cell wall-related genes, pectin-modifying genes, cellulose synthesis genes, and xyloglucan-modifying enzymes were particularly affected (Fig. 7C; Supplementary Fig. S14). Strikingly, the modifications observed were not linked to the softening genes active upon fruit ripening (*PG2A*, *β-GAL4*, *PL2*, and *EXP1*) but to cell wall-related genes expressed earlier during fruit development such as *XTH1*, *PAE-like*, and *CS-like*. The data support the view of the acquisition of a new metabolic differentiation program leading to a different cell wall structure which induces tissue softening at early stages of fruit development. Indeed, the expression of genes known to play a major role in cell wall degradation such as polygalacturonase, β-galactosidase, expansin, and pectate lyase *PL2* (Grierson *et al.*, 1986; Brummell *et al.*, 1999; Smith *et al.*, 2002; Uluisik *et al.*, 2016) was very limited during early development of *Sl-AGL11OE* fruit and therefore cannot account for the extreme softening already taking place in green fruits. In contrast, *XTH*, *PAE*, *PME*, and *Cellulose Synthase* displayed abnormal expression patterns in *Sl-AGL11OE* fruits and may be considered as promising candidates for green fruit-associated cell wall modifications. Indeed, *XTH* has been previously reported in different fleshy fruits such as pears, litchis, kiwis, apples, and strawberries to be associated with cell wall loosening (Miedes and Lorences, 2009). In tomato, heterologous expression of the *Sl-XTH1* tobacco homolog reduced softening (Miedes *et al.*, 2011). Several genes coding for pectin-modifying enzymes were also down-regulated in *Sl-AGL11OE* fruits including pectin methylesterases (Solyc06g009190, Solyc07g017600, Solyc12g009270, and Solyc03g123630) and a *PAE-like* gene (Solyc08g005800). The altered expression of these genes, notably those involved in pectin methylesterification, may contribute to the extreme softening of *Sl-AGL11OE* fruits since pectin modification usually occurs during the expansion phase of young fruits (Terao *et al.*, 2013). What is more, in the Arabidopsis class D MADS-box *stk* mutant, which displays abnormal differentiation of the cell wall matrix, the homeotic STK transcription factor directly controls a molecular network regulating cell wall properties in seed coats (Mizzotti *et al.*, 2014; Ezquer *et al.*, 2016). This network includes *AtPME16*, *Cellulose Synthase CESA5* and *CESA2*, *Cellulose Synthase-like CSLA2*, *COBRA-LIKE COBL2*, and *MYB61*. Interestingly, all the tomato closest homologs of these Arabidopsis genes (Solyc04g071650, Solyc10g083670, Solyc06g074630, Solyc11g066820, Solyc02g06577, and Solyc01g102340) were found to be differentially expressed in *Sl-AGL11OE* fruits (Supplementary Table S1). Taken together, both Arabidopsis *STK* and tomato *Sl-AGL11* class D MADS-box genes seem to control cell wall differentiation programs.

The conversion of sepal into an intermediary organ between leaf and fleshy carpel offers a model to decipher the early mechanisms involved in the acquisition of the fleshy character. The convergences and divergences between class C and *Sl-AGL11* emphasized here might provide a useful tool to evaluate the functional evolution and action modes of the *AGAMOUS* family of transcription factors. Implementation of ChIP-seq strategies might allow uncovering of the conserved target genes and provide clues as to how the different isoforms have acquired their specialization during flowering plant evolution. In that perspective, the functional characterization of *Sl-MBP3* becomes essential to complete the picture of the tomato class C/D MADS-box gene family. With a prospect of applications, the present study highlights the impact of *Sl-AGL11* on several fruit quality traits, notably the increase of sugar content and the modification of fruit firmness. Identifying the downstream components of *Sl-AGL11* will provide leads towards understanding the determinants of sink strength and fruit firmness, and might uncover new mechanisms controlling fruit quality and productivity that could ultimately be used in breeding programs.

Supplementary data

Supplementary data are available at *JXB* online.

Fig. S1. Phylogenetic tree of *AGAMOUS*-like MADS-box genes.

Fig. S2. Expression pattern of different MADS genes (*TAG1*, *TAGL1*, *Sl-AGL11*, *Sl-MBP3*, *RIN*) deduced from the RNA-Seq data.

Fig. S3. Subcellular localization of *Sl*-AGL11 protein.

Fig. S4. Morphology of nine independent tomato lines with RNAi-mediated down-regulation of *Sl-AGL11*.

Fig. S5. Ruthenium red and vanillin staining of seeds in the wild type (WT) and *Sl-AGL11*-RNAi line.

Fig. S6. Expression level of four *Agamous* genes in DPA10 fruits measured by qPCR.

Fig. S7. Plant size of S*l-AGL11OE* plants

Fig. S8. Flower phenotypes of *Sl-AGL11OE* lines.

Fig. S9. Abscission zone and pedicel swelling in an *Sl-AGL11OE* plant.

Fig. S10. Fruit size, fruit weight. and number of cell layers in pericarp of *Sl-AGL11*-overexpressing lines.

Fig. S11. Timing of flower initiation in WT and *Sl-AGL11OE* lines.

Fig. S12. Pollination efficiency of *Sl-AGL11*-overexpressing plants.

Fig. S13. Water loss and water content in tomato fruits overexpressing *Sl-AGL11*.

Fig. S14. MAPMAN enrichment of different functional categories in *Sl-AGL11OE* sepals and fruits.

Table S1. List of cell wall-related DEGs in *Sl-AGL11OE* versus WT fruit with known homologs affected in the Arabidopsis *STK* mutant

Table S2. List of primers used in this study

Data S1. Number of counts in RNA-Seq experiments performed on fruits and sepals harvested at the DPA10 stage.

Data S2. List of differentially expressed genes in the *Sl-AGL11OE* versus WT fruits harvested at the DPA10 stage.

Data S3. List of differentially expressed genes in the *Sl-AGL11OE* verusu WT sepals harvested at the DPA10 stage.

Acknowledgements

The authors are grateful to L. Lemonnier and D. Saint-Martin for the cultivation of tomato plants, to GetPlage for deep sequencing, and to GenoToulBioinfo for computing facilities. This research was supported by the Labex TULIP (ANR-10-LABX-41), by the TomGEM H2020 project, by the National Key Research and Development Program (2016YFD0400101), and by the National Natural Science Foundation of China (31572175). The work benefited from the networking activities within the European COST Action FA1106. BH was the beneficiary of the ERASMUS MUNDUS program.

Author contributions

BH performed the experiments and contributed to the drafting of the article; WD and ML helped in generating the transgenic lines; IM carried out sub-cellular localization experiments; JV and JG contributed to the writing and the critical analysis of the results; GH, MZ, EM, and PF contributed to the RNA-Seq experiment; JMR contributed to the RNA-Seq data processing, to the critical analysis, and the drafting of the manuscript; ZL, BVDR, and MB designed the study and wrote the manuscript.

References

Ampomah-Dwamena C, Morris BA, Sutherland P, Veit B, Yao JL. 2002. Down-regulation of TM29, a tomato SEPALLATA homolog, causes parthenocarpic fruit development and floral reversion. Plant Physiology **130,** 605–617.

Angenent GC, Franken J, Busscher M, van Dijken A, van Went JL, Dons HJ, van Tunen AJ. 1995. A novel class of MADS box genes is involved in ovule development in petunia. The Plant Cell **7,** 1569–1582.

Audran-Delalande C, Bassa C, Mila I, Regad F, Zouine M, Bouzayen M. 2012. Genome-wide identification, functional analysis and expression profiling of the Aux/IAA gene family in tomato. Plant and Cell Physiology **53,** 659–672.

Bemer M, Karlova R, Ballester AR, Tikunov YM, Bovy AG, Wolters-Arts M, Rossetto Pde B, Angenent GC, de Maagd RA. 2012. The tomato FRUITFULL homologs TDR4/FUL1 and MBP7/FUL2 regulate ethylene-independent aspects of fruit ripening. The Plant Cell **24,** 4437–4451.

Brummell DA, Harpster MH, Civello PM, Palys JM, Bennett AB, Dunsmuir P. 1999. Modification of expansin protein abundance in tomato fruit alters softening and cell wall polymer metabolism during ripening. The Plant Cell **11,** 2203–2216.

Colombo L, Franken J, Koetje E, van Went J, Dons HJ, Angenent GC, van Tunen AJ. 1995. The petunia MADS box gene FBP11 determines ovule identity. The Plant Cell **7,** 1859–1868.

Colombo L, Franken J, Van der Krol AR, Wittich PE, Dons HJ, Angenent GC. 1997. Downregulation of ovule-specific MADS box genes from petunia results in maternally controlled defects in seed development. The Plant Cell **9,** 703–715.

de Folter S, Shchennikova AV, Franken J, Busscher M, Baskar R, Grossniklaus U, Angenent GC, Immink RG. 2006. A Bsister MADS-box gene involved in ovule and seed development in petunia and Arabidopsis. The Plant Journal **47,** 934–946.

Deng W, Chen G, Peng F, Truksa M, Snyder CL, Weselake RJ. 2012. Transparent testa16 plays multiple roles in plant development and is involved in lipid synthesis and embryo development in canola. Plant Physiology **160,** 978–989.

Dong T, Hu Z, Deng L, Wang Y, Zhu M, Zhang J, Chen G. 2013. A tomato MADS-box transcription factor, SlMADS1, acts as a negative regulator of fruit ripening. Plant Physiology **163,** 1026–1036.

Dreni L, Kater MM. 2014. MADS reloaded: evolution of the AGAMOUS subfamily genes. New Phytologist **201,** 717–732.

Dreni L, Pilatone A, Yun D, Erreni S, Pajoro A, Caporali E, Zhang D, Kater MM. 2011. Functional analysis of all AGAMOUS subfamily members in rice reveals their roles in reproductive organ identity determination and meristem determinacy. The Plant Cell **23,** 2850–2863.

Earley KW, Haag JR, Pontes O, Opper K, Juehne T, Song K, Pikaard CS. 2006. Gateway-compatible vectors for plant functional genomics and proteomics. The Plant Journal **45,** 616–629.

Ecarnot M, Bączyk P, Tessarotto L, Chervin C. 2013. Rapid phenotyping of the tomato fruit model, Micro-Tom, with a portable VIS-NIR spectrometer. Plant Physiology and Biochemistry **70,** 159–163.

Ezquer I, Mizzotti C, Nguema-Ona E, *et al*. 2016. The developmental regulator SEEDSTICK controls structural and mechanical properties of the Arabidopsis seed coat. The Plant Cell **28,** 2478–2492.

Favaro R, Pinyopich A, Battaglia R, Kooiker M, Borghi L, Ditta G, Yanofsky MF, Kater MM, Colombo L. 2003. MADS-box protein complexes control carpel and ovule development in Arabidopsis. The Plant Cell **15,** 2603–2611.

Fujisawa M, Nakano T, Shima Y, Ito Y. 2013. A large-scale identification of direct targets of the tomato MADS box transcription factor RIPENING INHIBITOR reveals the regulation of fruit ripening. The Plant Cell **25,** 371–386.

Giménez E, Castañeda L, Pineda B, Pan IL, Moreno V, Angosto T, Lozano R. 2016. TOMATO AGAMOUS1 and ARLEQUIN/TOMATO AGAMOUS-LIKE1 MADS-box genes have redundant and divergent functions required for tomato reproductive development. Plant Molecular Biology **91,** 513–531.

Giménez E, Pineda B, Capel J, *et al*. 2010. Functional analysis of the Arlequin mutant corroborates the essential role of the ARLEQUIN/TAGL1 gene during reproductive development of tomato. PLoS One **5,** e14427.

Grierson D, Tucker GA, Keen J, Ray J, Bird CR, Schuch W. 1986. Sequencing and identification of a cDNA clone for tomato polygalacturonase. Nucleic Acids Research **14,** 8595–8603.

Hao Y, Hu G, Breitel D, Liu M, Mila I, Frasse P, Fu Y, Aharoni A, Bouzayen M, Zouine M. 2015. Auxin response factor SlARF2 is an essential component of the regulatory mechanism controlling fruit ripening in tomato. PLoS Genetics **11,** e1005649.

Heijmans K, Ament K, Rijpkema AS, Zethof J, Wolters-Arts M, Gerats T, Vandenbussche M. 2012. Redefining C and D in the petunia ABC. The Plant Cell **24,** 2305–2317.

Hu G, Fan J, Xian Z, Huang W, Lin D, Li Z. 2014. Overexpression of SlREV alters the development of the flower pedicel abscission zone and fruit formation in tomato. Plant Science **229,** 86–95.

Itkin M, Seybold H, Breitel D, Rogachev I, Meir S, Aharoni A. 2009. TOMATO AGAMOUS-LIKE 1 is a component of the fruit ripening regulatory network. The Plant Journal **60,** 1081–1095.

Karlova R, Chapman N, David K, Angenent GC, Seymour GB, de Maagd RA. 2014. Transcriptional control of fleshy fruit development and ripening. Journal of Experimental Botany **65,** 4527–4541.

Kater MM, Colombo L, Franken J, Busscher M, Masiero S, Van Lookeren Campagne MM, Angenent GC, Campagne MMVL, Angenent GC. 1998. Multiple AGAMOUS homologs from cucumber and petunia differ in their ability to induce reproductive organ fate. The Plant Cell **10,** 171–182.

Kempin SA, Mandel MA, Yanofsky MF. 1993. Conversion of perianth into reproductive organs by ectopic expression of the tobacco floral homeotic gene NAG1. Plant Physiology **103,** 1041–1046.

Langmead B, Salzberg SL. 2012. Fast gapped-read alignment with Bowtie 2. Nature Methods **9,** 357–359.

Leclercq J, Ranty B, Sanchez-Ballesta MT, *et al*. 2005. Molecular and biochemical characterization of LeCRK1, a ripening-associated tomato CDPK-related kinase. Journal of Experimental Botany **56,** 25–35.

Liljegren SJ, Ditta GS, Eshed Y, Savidge B, Bowman JL, Yanofsky MF. 2000. SHATTERPROOF MADS-box genes control seed dispersal in Arabidopsis. Nature **404,** 766–770.

Liu M, Diretto G, Pirrello J, Roustan JP, Li Z, Giuliano G, Regad F, Bouzayen M. 2014. The chimeric repressor version of an Ethylene Response Factor (ERF) family member, Sl-ERF.B3, shows contrasting effects on tomato fruit ripening. New Phytologist **203,** 206–218.

Love MI, Huber W, Anders S. 2014. Moderated estimation of fold change and dispersion for RNA-seq data with DESeq2. Genome Biology **15,** 550.

Lovisetto A, Baldan B, Pavanello A, Casadoro G. 2015. Characterization of an AGAMOUS gene expressed throughout development of the fleshy fruit-like structure produced by *Ginkgo biloba* around its seeds. BMC Evolutionary Biology **15,** 139.

Løvdal T, Lillo C. 2009. Reference gene selection for quantitative real-time PCR normalization in tomato subjected to nitrogen, cold, and light stress. Analytical Biochemistry **387,** 238–242.

Malabarba J, Buffon V, Mariath JEA, Gaeta ML, Dornelas MC, Margis-Pinheiro M, Pasquali G, Revers LF. 2017. The MADS-box gene Agamous-like 11 is essential for seed morphogenesis in grapevine. Journal of Experimental Botany **68,** 1493–1506.

Martel C, Vrebalov J, Tafelmeyer P, Giovannoni JJ. 2011. The tomato MADS-box transcription factor RIPENING INHIBITOR interacts with promoters involved in numerous ripening processes in a COLORLESS NONRIPENING-dependent manner. Plant Physiology **157,** 1568–1579.

Maza E. 2016. In papyro comparison of TMM (edgeR), RLE (DESeq2), and MRN normalization methods for a simple two-conditions-without-replicates RNA-seq experimental design. Frontiers in Genetics **7,** 164.

Maza E, Frasse P, Senin P, Bouzayen M, Zouine M. 2013. Comparison of normalization methods for differential gene expression analysis in RNA-Seq experiments: a matter of relative size of studied transcriptomes. Communicative and Integrative Biology **6,** e25849.

Mejía N, Soto B, Guerrero M, *et al*. 2011. Molecular, genetic and transcriptional evidence for a role of VvAGL11 in stenospermocarpic seedlessness in grapevine. BMC Plant Biology **11,** 57.

Mellway RD, Lund ST. 2013. Interaction analysis of grapevine MIKC(c)-type MADS transcription factors and heterologous expression of putative véraison regulators in tomato. Journal of Plant Physiology **170,** 1424–1433.

Miedes E, Lorences EP. 2009. Xyloglucan endotransglucosylase/hydrolases (XTHs) during tomato fruit growth and ripening. Journal of Plant Physiology **166,** 489–498.

Miedes E, Zarra I, Hoson T, Herbers K, Sonnewald U, Lorences EP. 2011. Xyloglucan endotransglucosylase and cell wall extensibility. Journal of Plant Physiology **168,** 196–203.

Mizukami Y, Ma H. 1992. Ectopic expression of the floral homeotic gene AGAMOUS in transgenic Arabidopsis plants alters floral organ identity. Cell **71,** 119–131.

Mizukami Y, Ma H. 1997. Determination of Arabidopsis floral meristem identity by AGAMOUS. The Plant Cell **9,** 393–408.

Mizzotti C, Ezquer I, Paolo D, *et al*. 2014. SEEDSTICK is a master regulator of development and metabolism in the Arabidopsis seed coat. PLoS Genetics **10,** e1004856.

Mizzotti C, Mendes MA, Caporali E, Schnittger A, Kater MM, Battaglia R, Colombo L. 2012. The MADS box genes SEEDSTICK and ARABIDOPSIS Bsister play a maternal role in fertilization and seed development. The Plant Journal **70,** 409–420.

Ng M, Yanofsky MF. 2001. Function and evolution of the plant MADS-box gene family. Nature Reviews. Genetics **2,** 186–195.

Ocarez N, Mejía N. 2016. Suppression of the D-class MADS-box AGL11 gene triggers seedlessness in fleshy fruits. Plant Cell Reports **35,** 239–254.

Pan IL, McQuinn R, Giovannoni JJ, Irish VF. 2010. Functional diversification of AGAMOUS lineage genes in regulating tomato flower and fruit development. Journal of Experimental Botany **61,** 1795–1806.

Pattison RJ, Csukasi F, Zheng Y, Fei Z, van der Knaap E, Catalá C. 2015. Comprehensive tissue-specific transcriptome analysis reveals distinct regulatory programs during early tomato fruit development. Plant Physiology **168,** 1684–1701.

Pinyopich A, Ditta GS, Savidge B, Liljegren SJ, Baumann E, Wisman E, Yanofsky MF. 2003. Assessing the redundancy of MADS-box genes during carpel and ovule development. Nature **424,** 85–88.

Pnueli L, Hareven D, Rounsley SD, Yanofsky MF, Lifschitz E. 1994. Isolation of the tomato AGAMOUS gene TAG1 and analysis of its homeotic role in transgenic plants. The Plant Cell **6,** 163–173.

Qin G, Wang Y, Cao B, Wang W, Tian S. 2012. Unraveling the regulatory network of the MADS box transcription factor RIN in fruit ripening. The Plant Journal **70,** 243–255.

Riechmann JL, Meyerowitz EM. 1997. Determination of floral organ identity by Arabidopsis MADS domain homeotic proteins AP1, AP3, PI, and AG is independent of their DNA-binding specificity. Molecular Biology of the Cell **8,** 1243–1259.

Seymour GB, Østergaard L, Chapman NH, Knapp S, Martin C. 2013. Fruit development and ripening. Annual Review of Plant Biology **64,** 219–241.

Shima Y, Fujisawa M, Kitagawa M, *et al*. 2014. Tomato FRUITFULL homologs regulate fruit ripening via ethylene biosynthesis. Bioscience, Biotechnology, and Biochemistry **78,** 231–237.

Singh R, Low ET, Ooi LC, *et al*. 2013. The oil palm SHELL gene controls oil yield and encodes a homologue of SEEDSTICK. Nature **500,** 340–344.

Smaczniak C, Immink RGH, Angenent GC, Kaufmann K. 2012. Developmental and evolutionary diversity of plant MADS-domain factors: insights from recent studies. Development **139,** 3081–3098.

Smith DL, Abbott JA, Gross KC. 2002. Down-regulation of tomato beta-galactosidase 4 results in decreased fruit softening. Plant Physiology **129,** 1755–1762.

Sonnewald U, Brauer M, von Schaewen A, Stitt M, Willmitzer L. 1991. Transgenic tobacco plants expressing yeast-derived invertase in either the cytosol, vacuole or apoplast: a powerful tool for studying sucrose metabolism and sink/source interactions. The Plant Journal **1,** 95–106.

Tadiello A, Pavanello A, Zanin D, Caporali E, Colombo L, Rotino GL, Trainotti L, Casadoro G. 2009. A PLENA-like gene of peach is involved in carpel formation and subsequent transformation into a fleshy fruit. Journal of Experimental Botany **60,** 651–661.

Terao A, Hyodo H, Satoh S, Iwai H. 2013. Changes in the distribution of cell wall polysaccharides in early fruit pericarp and ovule, from fruit set to early fruit development, in tomato (*Solanum lycopersicum*). Journal of Plant Research **126,** 719–728.

Thimm O, Bläsing O, Gibon Y, *et al*. 2004. MAPMAN: a user-driven tool to display genomics data sets onto diagrams of metabolic pathways and other biological processes. The Plant Journal **37,** 914–939.

Tomato Genome Consortium. 2012. The tomato genome sequence provides insights into fleshy fruit evolution. Nature **485,** 635–641.

Trapnell C, Pachter L, Salzberg SL. 2009. TopHat: discovering splice junctions with RNA-Seq. Bioinformatics **25,** 1105–1111.

Uluisik S, Chapman NH, Smith R, *et al*. 2016. Genetic improvement of tomato by targeted control of fruit softening. Nature Biotechnology **34,** 950–952.

Van Der Krol AR, Chua NH. 1993. Flower development in Petunia. The Plant Cell **5,** 1195–1203.

Vrebalov J, Pan IL, Arroyo AJ, *et al*. 2009. Fleshy fruit expansion and ripening are regulated by the tomato SHATTERPROOF gene TAGL1. The Plant Cell **21,** 3041–3062.

Vrebalov J, Ruezinsky D, Padmanabhan V, White R, Medrano D, Drake R, Schuch W, Giovannoni J. 2002. A MADS-box gene necessary for fruit ripening at the tomato ripening-inhibitor (rin) locus. Science **296,** 343–346.

Wang H, Jones B, Li Z, *et al*. 2005. The tomato Aux/IAA transcription factor IAA9 is involved in fruit development and leaf morphogenesis. The Plant Cell **17,** 2676–2692.

Xie Q, Hu Z, Zhu Z, Dong T, Zhao Z, Cui B, Chen G. 2014. Overexpression of a novel MADS-box gene SlFYFL delays senescence, fruit ripening and abscission in tomato. Scientific Reports **4,** 4367.

Xu W, Fiume E, Coen O, Pechoux C, Lepiniec L, Magnani E. 2016. Endosperm and nucellus develop antagonistically in Arabidopsis seeds. The Plant Cell **28,** 1343–1360.

Zhong S, Fei Z, Chen YR, *et al*. 2013. Single-base resolution methylomes of tomato fruit development reveal epigenome modifications associated with ripening. Nature Biotechnology **31,** 154–159.

Zouine M, Maza E, Djari A, Lauvernier M, Frasse P, Smouni A, Pirrello J, Bouzayen M. 2017. TomExpress, a unified tomato RNA-Seq platform for visualization of expression data, clustering and correlation networks. The Plant Journal Article DOI: 10.1111/tpj.13711.